$[Mo(XC_6H_4CSN_2)(XC_6H_4CSN_2H)(XC_6H_4CSNNCMe_2)] \underset{}{\overset{1e^-}{\rightleftharpoons}}$

$$[Mo(XC_6H_4CSN_2)(XC_6H_4CSN_2H)(XC_6H_4CSNNCMe_2)]^- \quad (1)$$

Figure 8. Effect of substituents on the primary cathodic couple $[Mo(XC_6H_4CSN_2)(XC_6H_4CSN_2H)(XC_6H_4CSNNCMe_2)]/[Mo-(XC_6H_4CSN_2)(XC_6H_4CSN_2H)(XC_6H_4CSNNCMe_2)]^-$. Relationship between the reduction potential and the Hammett constant σ_p^n.[40]

unsubstituted precursors $[Mo(XC_6H_4CSN_2H)_3]$, as shown in Table X and Figure 7. The initial cathodic process is quasi-reversible, the degree of reversibility dependent on the aryl substituent. The electrode process is described by eq 1. The reduction product has been generated by controlled potential electrolysis in an EPR tube, yielding a one-line spectrum centered at $g = 2.01$. The substituent effect on the reversible one-electron reduction is illustrated in Figure 8. The correlation with σ_p^n establishes that the trend is related to simple inductive effects. Thus, the more electron-withdrawing groups stabilize the reduced form relative to the neutral complex and

yield more positive redox potentials for the reductive couple. Conversely, the electron-donating methyl substituent provides the most negative redox potential. A similar substituent dependence of redox potential has been observed in the electrochemical oxidation of the complexes $[Mo-(N_2C_6H_4X)(S_2CNR_2)_3]$.[44]

A number of successive irreversible cathodic processes occur in the range -1.5 to -2.0 V for the hydrazonido derivatives. The nature of these processes has not been established, controlled potential electrolysis at these potentials yielding nonintegral values for electrons transferred and producing insoluble materials.

Supplementary Material Available: Listings of calculated and observed structure factors (65 pages). Ordering information is given on any current masthead page.

(44) Butler, G.; Chatt, J.; Leigh, G. J.; Pickett, C. J. *J. Chem. Soc., Dalton Trans.* **1971**, 13.

Contribution from the Department of Chemistry,
Wayne State University, Detroit, Michigan 48202

Crystal and Molecular Structure of Tricyclopropylaluminum Dimer

W. H. ILSLEY, M. D. GLICK, JOHN P. OLIVER,* and J. W. MOORE

The crystal and molecular structure of tricyclopropylaluminum dimer has been determined at 22 °C and at -62 °C. The molecule crystallizes in the space group $P2_1/c$ with four molecules per unit cell. The cell dimensions are $a = 14.573$ (3) Å, $b = 9.422$ (2) Å, $c = 13.719$ (6) Å, $\beta = 98.12$ (2)°, and $V = 1864.8$ Å^3 at 22 °C and $a = 14.470$ (2) Å, $b = 9.319$ (2) Å, $c = 13.431$ (2) Å, $\beta = 99.06$ (1)°, and $V = 1788.5$ (5) Å^3 at -62 °C. Conventional discrepancy factors of 0.091 at 22 °C and 0.072 at -62 °C were obtained for a disordered model. The observed bond distances show normal Al–C terminal distances (1.944 Å average) and normal bridge Al–C distances (2.074 Å average). Both the terminal and bridging cyclopropyl groups have relatively long C_α–C_β bonds and short C_β–C_β bond distances. The severe distortion of the longer C–C distances observed in the bridging cyclopropyl groups are interpreted in terms of nonbonding metal orbital α-carbon p-orbital overlap yielding increased stability for the cyclopropyl-bridged aluminum dimer.

Introduction

The structures of organoaluminum derivatives have been of great interest over the years because of the early discovery that these systems contain bridging, five-coordinate carbon atoms. Since the initial work several structural determinations have been carried out with most of these recently reviewed in detail.[1] The solid-state structures determined include Al_2Me_6,[2] $Ph_2NAl_2Me_5$,[3] Al_2Ph_6,[4] $Al_2Ph_2Me_4$,[5] $Al_2(\mu\text{-}trans\text{-}CH{=}CH\text{-}(t\text{-}Bu))_2(i\text{-}Bu)_4$,[6] and preliminarily reported $Al_2(\mu\text{-}C{\equiv}CPh)_2Ph_4$[7] and $Al_2(c\text{-}Pr)_6$.[8] In addition, the structure of

$Al_2(C{\equiv}C\text{-}Me)_2Me_4$ determined in the gas phase has recently appeared.[9] Prior to these structural determinations a bonding model was proposed on the basis of the unusual stability of the bridged dimer Ga_2Vi_6,[10] which involved the overlap of the hybrid orbital of the bridging carbon atom with the two metal orbitals, as suggested for Al_2Me_6, with additional stabilization arising from the interaction of the π system with the vacant nonbonding orbitals centered on the metal atom. This model has since been extended to account for the stability of the vinyl-bridged aluminum compounds,[11] of the arylaluminum

(1) Oliver, J. P. *Adv. Organomet. Chem.* **1977**, *16*, 131.
(2) Lewis, P. H.; Rundle, R. E. *J. Chem. Phys.* **1953**, *21*, 987. Vranka, R. G.; Amma, E. L. *J. Am. Chem. Soc.* **1967**, *89*, 3121. Huffman, J. C. C.; Streib, W. E. *J. Chem. Soc. D* **1971**, 911.
(3) Magnuson, V. R.; Stucky, G. D. *J. Am. Chem. Soc.* **1968**, *90*, 3269.
(4) Malone, J. F.; McDonald, W. S. *Chem. Commun.* **1967**, 444. Malone, J. F.; McDonald, W. S. *J. Chem. Soc., Dalton Trans.* **1972**, 2646.
(5) Malone, J. F.; McDonald, W. S. *J. Chem. Soc. D* **1970**, 280. Malone, J. F.; McDonald, W. S. *J. Chem. Soc., Dalton Trans.* **1972**, 2649.
(6) Albright, M. J.; Butler, W. M.; Anderson, T. J.; Glick, M. D.; Oliver, J. P. *J. Am. Chem. Soc.* **1976**, *98*, 3995.
(7) Stucky, G. D.; McPherson, A. M.; Rhine, W. E.; Eisch, J. J.; Considine, J. L. *J. Am. Chem. Soc.* **1974**, *96*, 1941.
(8) Moore, J. W.; Sanders, D. A.; Scherr, P. A.; Glick, M. D.; Oliver, J. P. *J. Am. Chem. Soc.* **1971**, *93*, 1035.
(9) Almenningen, A.; Firnholt, L.; Haaland, A. *J. Organomet. Chem.* **1978**, *155*, 245.
(10) Oliver, J. P.; Stevens, L. G. *J. Inorg. Nucl. Chem.* **1962**, *21*, 137. Visser, H. D.; Oliver, J. P. *J. Am. Chem. Soc.* **1968**, *90*, 3579.

Table I. Lattice Parameters for $Al_2(c\text{-Pr})_6$

T, °C	22	-62
space group	$P2_1/c$	$P2_1/c$
a, Å	14.573 (3)	14.470 (2)
b, Å	9.422 (2)	9.319 (2)
c, Å	13.719 (6)	13.431 (2)
β, deg	98.12 (2)	99.06 (1)
Z	4	4
V, Å³	1864.8	1788.6 (5)
ρ_{calcd}, g/cm³	1.016	1.059

compounds,[12] and of the cyclopropyl-bridged species.[13] The subsequent structural data, cited earlier, support this model. The same model was suggested for the ethynyl-bridged derivatives.[14] However, on the basis of the structural data, a different model has been proposed[7] which involves an unsymmetrical bridge with an Al–C σ bond to one Al atom while the bridge is completed by formation of a bond between the π electrons and the vacant orbital of the second Al atom. This model is in accord with both ethynylaluminum structures which have been reported.[7,9]

We now wish to present a complete report on the structure of $Al_2(c\text{-Pr})_6$ determined at 22 °C and at -62 °C by single-crystal X-ray diffraction techniques. Further we wish to discuss the implications of the structures with regard to the proposed bonding models and exchange processes discussed elsewhere.

Experimental Section

The tricyclopropylaluminum dimer was prepared by the reaction of $Hg(c\text{-Pr})_2$ with aluminum metal as previously described.[13] The crystals used for data collection were obtained by vacuum sublimation and were mounted in thin-walled capillary tubes under an argon atmosphere in a drybox and sealed.

X-ray Data Collection for [Al(c-Pr)₃]₂. Room Temperature. The crystal used for data collection had dimensions 0.51 mm × 0.44 mm × 0.44 mm. Precession and cone-axis photographs taken with Mo Kα radiation ($\lambda = 0.71069$ Å) displayed monoclinic symmetry with the systematic absences $0k0$, $k = $ odd, and $h0l$, $l = $ odd. Consequently, the compound was unambiguously assigned to the space group $P2_1/c$ ($Z = 4$). Preliminary lattice constants were obtained by least-squares refinement of 16 reflections whose angles were accurately determined on a Picker four-circle, automatic diffractometer using Cu Kα_1 radiation ($\lambda = 1.5405$ Å). The lattice constants are summarized in Table I.

The data were collected on the Picker diffractometer, with Cu Kα radiation by using a moving crystal–moving counter (θ–2θ) scan technique. A scan of 3.0° corrected for Kα_1–Kα_2 separation was used for all reflections. The first 600 reflections were collected by using a scan rate of 1.0 °/min and stationary-background counts of 15 s. The remainder of the data were collected with a scan rate of 2.0 °/min and stationary-background counts of 10 s. The changes in scan and background rates were instituted to decrease the data collection time as the crystal appeared to be decomposing on irradiation. A 2-mil nickel foil was employed to filter the Cu Kβ radiation. All reflections whose peak intensities were greater than 10 000 counts/s were attenuated with variable-thickness brass foils.

A total of 2891 independent reflections in the $\pm hkl$ quadrant were collected to a maximum $2\theta = 120°$. After these data were collected, crystal movement and decomposition became intolerable and data collection was terminated. Four standards were monitored every 97 reflections. The standards showed a net decrease of $\sim$26% during the course of data collection. The data were corrected in a stepwise fashion in blocks of 100 reflections.

The intensity data were then corrected for Lorentz and polarization effects. Standard deviations were assigned to the F^2's according to the formula

$$\sigma(I) = \left[P + \left(\frac{B}{B_1 + B_2} \right) + \left(\frac{B_1 + B_2}{30(SR)(TB)} \right)^2 (2\sigma(2\theta)) + \right.$$
$$\left. (I(\sigma(A)/A))^2 + (I(\sigma(S)/S))^2 + ((PIC)I)^2 \right]^{1/4}$$

where P is the integrated intensity, B_1 and B_2 are the background counts, I is the net intensity, SR is the scan rate, TB is the background counting time, S is the scale factor, A is the attenuator factor, PIC is an "ignorance factor", and B is given by

$$B = 30[(|2\theta_2 - 2\theta_1|)/(SR)(TB)](B_1 + B_2)$$

An ignorance factor of 0.05 and a $\sigma(2\theta)$ of 0.0025° were used. Of the 2891 reflections collected, 1887 had $I \geq 3.0\sigma(I)$. The $\sigma(I)$'s obtained when the power of $^1/_2$ is used in the above formula gave unrealistically low $\sigma(F^2)$'s for the high-intensity data. Consequently, the high-intensity reflections were underweighted in the least-squares refinement. By use of the exponential power of $^1/_4$ the high-intensity reflections were given more weight in the refinement and a lower discrepancy value was obtained.

Low Temperature. The crystal chosen for data collection was of dimensions 0.49 mm × 0.46 mm × 0.32 mm. The crystal was sealed under argon in a thin-walled capillary and mounted on a Syntex $P2_1$ four-circle diffractometer with an LT-1 low-temperature attachment. An initial orientation matrix was established at room temperature by centering on 15 reflections with 2θ between 5 and 18°, whose positions were determined from a rotation photograph. The temperature was then lowered to -62 °C, and an accurate orientation matrix was established by centering on 15 reflections (Mo Kα; $\lambda = 0.71069$ Å) with 2θ between 24 and 31° that were obtained from a preliminary data scan of the $\pm hkl$ quadrant. The observed lattice constants are given in Table I. This temperature was chosen since no significant increase was observed in the intensities of selected reflections below this temperature. The data were collected in the θ–2θ mode with Mo Kα radiation at a scan rate of 2°/min and a scan range of K$\alpha_1 = -1.0$ to K$\alpha_2 = +1.0$. A total of 2653 independent reflections were collected in the $\pm hkl$ quadrant to a maximum 2θ equal to 50°. Standard deviations of intensities were assigned as

$$\sigma(I) = [\sigma_{counter}I^2 + (0.04I)^2]^{1/2}$$

where $\sigma_{counter} = (I + K^2B)^{1/2}$, I is the net intensity, B is the total background counting time, and K is the ratio of scan time to background counting time. Background counts were taken for half the scan time. Three standard reflections were monitored every 97 reflections as a check on crystal and electronic stability. The standards showed no significant decrease in intensity throughout data collection. Of the 2653 data collected, there were 1789 reflections with $I \geq 2.5\sigma(I)$ which were used in solving the structure.

Solution and Refinement of [Al(c-Pr)₃]₂. Room Temperature. Application of the Patterson function yielded the positions of the two aluminum atoms. Independent application of the Sayre relation yielded the same positions. Subsequent three-dimensional Fourier and difference syntheses gave the positions of the remaining nonhydrogen atoms and after six cycles of full-matrix isotropic refinement gave discrepancy factors of

$$R_1 = \sum ||F_o| - |F_c||-\sum |F_o| = 0.166$$
$$R_2 = [\sum w(|F_o| - |F_c|)^2/\sum w|F_o|^2]^{1/2} = 0.202$$

Idealized hydrogen positions were then calculated with[15] each hydrogen being assigned an isotropic thermal parameter equivalent to the thermal parameter of the carbon atom to which it was bound. Two cycles of full-matrix isotropic refinement, followed by four cycles of full-matrix anisotropic least-squares refinement with fixed contributions for the hydrogen atoms, resulted in final discrepancy factors of R_1

(11) Zweifel, G.; Clark, G. M. *J. Organomet. Chem.* **1972**, *39*, C33. Clark, C. M.; Zweifel, G. *J. Am. Chem. Soc.* **1971**, *93*, 527.

(12) Henold, K. L.; Oliver, J. P. *Organomet. React.* **1975**, *5*, 387.

(13) Oliver, J. P.; Sanders, D. A. *J. Am. Chem. Soc.* **1968**, *90*, 5910. Sanders, D. A.; Scherr, P. A.; Oliver, J. P. *Inorg. Chem.* **1976**, *15*, 861.

(14) Mole, T.; Jeffery, E. A. "Organoaluminum Compounds"; Elsevier: Amsterdam, 1972; pp 275–278.

(15) Local versions of the following programs were used: (1) DACOR, D. Smith's program for data reduction; (2) SYNCOR, W. Schmonsees' program for data reduction; (3) NEWES, W. Schmonsees' program for generation of normalized structure factors; (4) REL, R. E. Long's program for phase determination by Sayre's method; (5) FORDAP, A. Zalkin's Fourier program; (6) ORFLS and ORFFE, W. Busing, K. Martin, and H. Levy's full-matrix least-squares program and function and error program; (7) ORTEP, C. K. Johnson's program for drawing crystal models; (8) HFINDR, A. Zalkin's idealized hydrogen program.

= 0.091 and R_2 = 0.119 with an error of fit of 7.32. The resulting thermal parameters were representative of large thermal motion or disorder.

Low Temperature. Starting positions for the Al atoms were taken to be those found for the structure at room temperature. The remaining nonhydrogen positions were determined from subsequent Fourier and difference syntheses. The carbon atom positions for five of the cyclopropyl groups were found relatively easily. The carbon atom positions for the remaining cyclopropyl group could not be determined accurately. The group was found to be severely disordered, and attempts to approximate this disorder by a number of models involving partial atoms failed. The largest peak in a difference map corresponded to the α-carbon of this ring (C(13)); the next three peaks corresponded to partially occupied positions for the β-carbons. Partial occupancy factors for these three positions (C(X), C(Y), C(Z)) were varied. Subsequent full-matrix anisotropic least-squares refinement on all the nonhydrogen atoms yielded discrepancy factors R_1 = 0.106 and R_2 = 0.146. The positions of the hydrogen atoms were then located from subsequent difference syntheses. Full-matrix anisotropic least-squares refinement of the nonhydrogen parameters (including occupancy factors where appropriate) and isotropic refinement of the hydrogen atom positions and thermal parameters yielded final discrepancy factors of R_1 = 0.072 and R_2 = 0.093, an error of fit of 2.77, and a residual electron density in the final difference maps of 0.71 e/Å^3. Table II gives the atomic coordinates and thermal parameters, and all bond distances and angles are presented in Table III. A listing of observed and calculated structure factors and amplitudes is available as supplementary material.

Results and Discussion

The structure of dimeric tricyclopropylaluminum is shown in Figure 1, and from this it is quite clear that the gross structural features of this dimer are similar to those observed in the other known bridged organoaluminum compounds. A comparison of several of the significant structural parameters for the known dimeric aluminum species is presented in Table IV for comparison.

The most striking feature in the structure of the cyclopropyl derivative is that the two bridging rings are on the same side of the cyclic Al–C–Al–C ring system in the syn conformation. This is in contrast to the anti conformation observed for the bridging units in bis(μ-(*trans-tert*-butylvinyl))-tetraisobutyl-dialuminum.[6] The difference in the orientation of the bridging groups most likely results from the different requirirements of the substituent group which alters the intramolecular repulsions between bridging and terminal moieties. The syn configuration also predominates in solution as indicated from ¹H NMR studies, even though CNDO II calculations suggest that the syn and anti configurations for the bridging cyclopropyl groups should be the same energy—at least when the terminal sites are occupied by methyl groups.[13]

The two terminal groups which lie on the same side of the Al–C–Al–C ring as the bridging groups are pointed away from the bridging moieties to minimize steric interactions. These rings are quite well-defined and show the C_α–C_β bonds longer than the C_β–C_β bonds. The Al–C terminal bond distances are normal for these two units as well as for the other two terminal cyclopropyl groups as seen in Table III.

The positions of the other terminal groups show that they are not constrained to the same extent and that they are not nearly as well-defined. In fact, one of these groups could not be completely located from either the room-temperature or the low-temperature X-ray data despite repeated efforts using several partial occupancy models. The high-thermal motion and/or existence of several orientations for this group indicate that it is relatively free to move even in the solid state. This thermal motion and the observed structure are completely compatible with the NMR studies conducted in this laboratory which indicate that the bridging rings prefer the syn configuration and are locked into this position on the NMR time scale at low temperature.[13,16] Further, these variable-tem-

perature NMR studies have been interpreted in terms of four types of processes, the high-temperature bridge–terminal exchange, low-temperature (down to –75 °C) rotation of the bridging groups, and fast rotation of the terminal groups on the same side as the bridging groups down to ~–90°, with rapid rotation of the other terminal groups even below this temperature. This interpretation differs from that of Olah et al.,[17] who have suggested that the terminal groups are frozen into a single conformation at temperatures of ~–75 °C with free rotation of the bridging groups occurring at lower temperatures. This latter interpretation does not appear to be compatible with NMR data previously obtained in this laboratory[13,16] nor is it consistent with the observed structure in the solid state.

Examination of Table IV reveals that the Al–C–Al angles in bridged-aluminum compounds range 75–79° and that the C_b–Al–C_b angles are in the range of 94–104° with Al–Al distances from 2.6–2.7 Å. Since these terms are all interrelated, it is not possible to make any meaningful correlations from the small and apparently random variations in them. It is interesting to note that in several of the bridged-aluminum derivatives for which structural data are available puckering

of the Al–C–Al–C ring occurs with the largest deviation from planarity occurring in the cyclopropyl system. Diagrams **1** and **2** show the dihedral angles between the two Al–C–Al
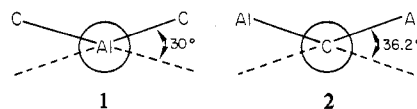
planes and the two C_b–Al–C_b planes, respectively. As noted earlier the syn orientation of the bridging groups and the puckered nature of this system most likely result from the various intramolecular interactions.

Examination of the various bond distances in Tables III and IV shows that the Al–C_b bond distances average 2.074 Å (–62 °C) and that this is the smallest Al–C_b distance reported for these symmetrical derivatives. This, however, may not be significant in view of the relatively small differences observed and the imprecise nature of the data. The C–C distances in the bridging cyclopropyl rings show far more variation, with the average C_α–C_β distance equal to 1.548 Å and the average C_β–C_β distance equal to 1.437 Å giving a difference of 0.111 Å for these C–C bond distances. This is clearly greater than 3σ and can be considered significant. Comparison with the corresponding distances observed for the three well-defined terminal groups, which have average distances C_α–C_β = 1.507 Å and C_β–C_β = 1.463 Å with a difference of 0.044 Å, shows that there is significant increase in the C_β–C_β distances, and a decrease in the C_α–C_β distances in the bridged cyclopropyl group when compared to those of the terminal groups. In addition these differences are large when compared to those of a variety of simple cyclopropyl derivatives,[18] which have values near that observed in cyclopropane (1.51 Å) and exceed

(16) In addition to the ¹H NMR data cited, preliminary studies using ¹³C FT NMR techniques on natural-abundance samples have confirmed the chemical shifts assigned by Olah et al.,[17] but the observed temperature dependence of the relaxation times indicates that the variable-temperature studies originally reported were misinterpreted: Thomas, R. D.; Oliver, J. P., unpublished observations.

(17) Olah, G. A.; Prakash, G. K. S.; Liang, G.; Henold, K. L.; Haigh, G. B. *Proc. Natl. Acad. Sci. U.S.A.* **1977**, *74*, 5217.

(18) For additional data and discussion of bond distances, see, for example: Saengen, W.; Schwalbe, C. H. *J. Org. Chem.* **1971**, *36*, 3401. Meester, M. A. M.; Schenk, H.; MacGillavry, C. H. *Acta Crystallogr., Sect. B* **1971**, *B27*, 630. Luhan, P. A.; McPhail, A. T. *J. Chem. Soc., Perkin Trans. 2* **1972**, 2372. Schwendeman, R. H.; Jacobs, G. D.; Krigas, T. M. *J. Chem. Phys.* **1964**, *40*, 1022. Bastiansen, O.; Fritsch, F. N.; Hedberg, K. *Acta Crystallogr.* **1964**, *17*, 538. Eraker, J.; Romming, C. *Acta Chem. Scand.* **1967**, *21*, 2721. Long, R. E.; Maddox, H.; Trueblood, K. N. *Acta Crystallogr., Sect. B* **1969**, *B25*, 2083.

Table II. Atomic Coordinates and Anisotropic Thermal Parameters[a,b] for $[Al(c-Pr)_3]_2$ Obtained at $-62\,^{\circ}C$

atom	x	y	z	occupancy factor	B_{iso}, A^2
Al(1)	0.6865 (1)	0.2558 (2)	0.6206 (1)		
Al(2)	0.8029 (1)	0.0408 (2)	0.6313 (1)		
C(1)	0.6707 (4)	0.0477 (6)	0.6712 (5)		
C(2)	0.6270 (5)	0.0727 (8)	0.7686 (5)		
C(3)	0.6881 (5)	−0.0513 (7)	0.7659 (5)		
C(4)	0.7850 (4)	0.2124 (8)	0.5286 (5)		
C(5)	0.8862 (6)	0.2447 (13)	0.5171 (7)		
C(6)	0.8261 (6)	0.3641 (12)	0.5188 (7)		
C(7)	0.7255 (4)	0.3944 (7)	0.7274 (5)		
C(8)	0.7080 (7)	0.5530 (9)	0.7050 (9)		
C(9)	0.6503 (7)	0.4760 (11)	0.7648 (11)		
C(10)	0.5720 (5)	0.3030 (8)	0.5302 (6)		
C(11)	0.4769 (5)	0.2496 (9)	0.5443 (7)		
C(12)	0.5175 (5)	0.2026 (9)	0.4551 (7)		
C(13)	0.8077 (6)	−0.1361 (10)	0.5579 (7)		
C(X)	0.8595 (10)	−0.1370 (16)	0.4613 (9)	0.84 (4)	
C(Y)	0.7624 (13)	−0.1981 (19)	0.4782 (15)	0.65 (3)	
C(16)	0.9023 (4)	0.0859 (7)	0.7436 (5)		
C(17)	0.9461 (4)	−0.0286 (9)	0.8166 (6)		
C(18)	1.0004 (5)	0.0299 (9)	0.7420 (6)		
C(Z)	0.8789 (7)	−0.2217 (12)	0.5375 (12)	1.00 (4)	
H(1)	0.6201 (32)	0.0042 (50)	0.6203 (36)		−1.3 (9)
H(2)	0.5604 (48)	0.0512 (70)	0.7622 (50)		2.3 (16)
H(3)	0.6473 (46)	0.1530 (80)	0.8046 (52)		2.0 (18)
H(4)	0.7461 (38)	−0.0480 (57)	0.8104 (40)		−0.3 (11)
H(5)	0.6575 (38)	−0.1402 (67)	0.7538 (42)		0.2 (12)
H(6)	0.7533 (37)	0.1801 (60)	0.4688 (46)		0.2 (12)
H(7)	0.9266 (40)	0.2103 (61)	0.5623 (47)		−0.2 (13)
H(8)	0.9047 (45)	0.2252 (75)	0.4492 (58)		2.4 (17)
H(9)	0.8062 (63)	0.4001 (99)	0.4545 (74)		5.6 (26)
H(10)	0.8333 (50)	0.4240 (80)	0.5804 (63)		2.9 (20)
H(11)	0.7826 (38)	0.3738 (62)	0.7788 (43)		0.5 (12)
H(12)	0.7528 (44)	0.6253 (75)	0.7469 (50)		2.1 (16)
H(13)	0.6875 (49)	0.5843 (83)	0.6495 (55)		1.8 (20)
H(14)	0.5795 (65)	0.4545 (91)	0.7318 (66)		5.4 (23)
H(15)	0.6566 (48)	0.4990 (79)	0.8167 (47)		−0.5 (17)
H(16)	0.5788 (39)	0.3794 (69)	0.5061 (45)		0.1 (14)
H(17)	0.4741 (38)	0.1853 (66)	0.6041 (47)		0.5 (13)
H(18)	0.4300 (49)	0.3190 (78)	0.5324 (56)		2.6 (18)
H(19)	0.5424 (37)	0.1010 (66)	0.4633 (42)		−0.1 (12)
H(20)	0.4878 (57)	0.2393 (95)	0.3796 (70)		5.7 (23)
H(26)	0.8991 (35)	0.1774 (63)	0.7690 (40)		−0.3 (12)
H(27)	0.9229 (41)	−0.1205 (77)	0.8043 (49)		1.3 (16)
H(28)	0.9589 (50)	0.0029 (84)	0.8792 (59)		2.7 (20)
H(29)	1.0118 (44)	−0.0182 (70)	0.6807 (53)		1.4 (15)
H(30)	1.0461 (41)	0.0913 (64)	0.7701 (45)		0.4 (13)

atom	B_{11}	B_{22}	B_{33}	B_{12}	B_{13}	B_{23}
Al(1)	2.2 (1)	2.2 (1)	2.5 (1)	−0.5 (1)	−0.3 (1)	0.5 (1)
Al(2)	2.3 (1)	2.6 (1)	2.2 (1)	−0.3 (1)	0.5 (1)	−0.6 (1)
C(1)	2.5 (2)	1.7 (3)	2.2 (3)	−0.3 (2)	−0.1 (2)	−0.1 (2)
C(2)	2.7 (3)	3.1 (4)	3.2 (3)	−0.3 (3)	1.4 (3)	0.2 (3)
C(3)	3.1 (3)	1.8 (3)	3.6 (3)	−0.2 (3)	−0.0 (3)	0.7 (3)
C(4)	2.8 (3)	5.6 (4)	1.5 (3)	−2.2 (3)	−0.6 (2)	0.7 (3)
C(5)	2.9 (4)	10.7 (7)	2.9 (4)	−2.2 (5)	−0.1 (3)	2.1 (5)
C(6)	3.9 (4)	7.8 (6)	3.5 (5)	−2.4 (4)	−0.2 (3)	2.6 (5)
C(7)	2.5 (3)	2.1 (3)	3.4 (3)	0.1 (2)	−0.1 (2)	0.2 (3)
C(8)	6.9 (5)	2.0 (4)	6.8 (6)	−0.1 (4)	−2.6 (5)	0.7 (4)
C(9)	4.5 (5)	4.0 (5)	10.7 (9)	0.5 (4)	0.9 (6)	−3.7 (6)
C(10)	4.1 (3)	2.3 (3)	5.1 (4)	−1.1 (3)	−1.0 (3)	1.7 (3)
C(11)	2.7 (3)	4.2 (4)	6.1 (5)	−0.3 (3)	−0.6 (3)	1.6 (4)
C(12)	3.3 (3)	4.6 (5)	4.4 (4)	−1.2 (3)	−1.0 (3)	1.2 (4)
C(13)	3.8 (4)	7.5 (6)	8.4 (6)	−2.9 (4)	3.2 (4)	−5.9 (5)
C(X)	11.0 (12)	8.4 (10)	3.8 (6)	5.8 (8)	2.5 (6)	0.8 (6)
C(Y)	7.6 (12)	9.3 (13)	11.1 (14)	1.9 (9)	−1.1 (10)	−5.3 (11)
C(16)	3.3 (3)	1.8 (3)	2.7 (3)	0.8 (2)	0.4 (2)	−0.0 (3)
C(17)	2.5 (3)	3.2 (4)	3.9 (4)	0.6 (3)	0.2 (3)	0.2 (3)
C(18)	1.9 (3)	5.1 (4)	4.0 (4)	0.1 (3)	−0.2 (3)	−0.1 (4)
C(Z)	7.5 (7)	5.8 (7)	12.0 (12)	1.9 (5)	1.0 (6)	−1.2 (7)

[a] Standard deviations from the variance–covariance matrix are given in parentheses for the least significant digit(s). [b] The form of the anisotropic temperature factor used was $\exp[-(h^2\beta_{11} + k^2\beta_{22} + l^2\beta_{33} + 2hk\beta_{12} + 2hl\beta_{13} + 2kl\beta_{23})]$. The values reported above are B's derived from the β's.

Table III. Interatomic Distances (Å) and Angles (Deg) for $Al_2(c\text{-Pr})_6$

	22 °C	−62 °C		22 °C	−62 °C
Al(1)-Al(2)	2.618 (3)	2.607 (3)	C(8)-C(9)	1.47 (1)	1.439 (15)
Al(1)-C(1)	2.063 (7)	2.080 (6)	C(10)-C(11)	1.48 (1)	1.503 (10)
Al(1)-C(4)	2.098 (7)	2.069 (7)	C(10)-C(12)	1.47 (1)	1.504 (10)
Al(2)-C(1)	2.090 (7)	2.068 (6)	C(11)-C(12)	1.48 (1)	1.480 (11)
Al(2)-C(4)	2.098 (8)	2.101 (7)	C(16)-C(17)	1.53 (1)	1.518 (9)
Al(1)-C(7)	1.947 (7)	1.947 (6)	C(16)-C(18)	1.51 (1)	1.516 (9)
Al(1)-C(10)	1.94 (1)	1.943 (7)	C(17)-C(18)	1.48 (1)	1.471 (10)
Al(2)-C(13)	1.90 (1)	1.928 (8)	C(1)-C(4)		3.124 (9)
Al(2)-C(16)	1.936 (8)	1.959 (6)	C(13)-C(14)	1.30 (1)	
C(1)-C(2)	1.56 (1)	1.558 (9)	C(13)-C(15)	1.22 (1)	
C(1)-C(3)	1.55 (1)	1.559 (8)	C(14)-C(15)	1.29 (1)	
C(2)-C(3)	1.47 (1)	1.459 (9)	C(13)-C(X)		1.598 (14)
C(4)-C(5)	1.54 (1)	1.527 (9)	C(13)-C(Y)		1.299 (17)
C(4)-C(6)	1.55 (1)	1.547 (12)	C(13)-C(Z)		1.364 (12)
C(5)-C(6)	1.47 (1)	1.414 (14)	C(X)-C(Y)		1.565 (21)
C(7)-C(8)	1.51 (1)	1.521 (10)	C(X)-C(Z)		1.288 (14)
C(7)-C(9)	1.51 (1)	1.479 (11)	C(Y)-C(Z)		1.761 (20)
C(4)-Al(1)-C(1)	97.5 (3)	97.7 (3)	C(17)-C(16)-C(18)	58.7 (5)	58.0 (4)
C(7)-Al(1)-C(1)	114.3 (3)	114.3 (3)	C(16)-C(18)-C(17)	61.4 (5)	61.0 (4)
C(10)-Al(1)-C(4)	105.4 (3)	105.7 (3)	C(16)-C(17)-C(18)	59.9 (5)	60.9 (5)
C(7)-Al(1)-C(10)	115.2 (4)	115.5 (3)	C(7)-Al(1)-C(4)	114.1 (3)	115.0 (2)
C(4)-Al(2)-C(1)	96.7 (3)	97.1 (2)	C(10)-Al(1)-C(1)	108.6 (3)	106.8 (3)
C(4)-Al(2)-C(16)	111.5 (3)	110.0 (3)	C(16)-Al(2)-C(1)	113.7 (3)	113.0 (3)
C(1)-Al(2)-C(13)	106.1 (5)	105.5 (3)	C(13)-Al(2)-C(4)	108.4 (5)	109.0 (4)
C(13)-Al(2)-C(16)	118.2 (5)	119.8 (4)	Al(1)-C(1)-C(3)	143.7 (5)	143.8 (4)
Al(1)-C(1)-Al(2)	78.2 (3)	77.9 (2)	Al(2)-C(1)-C(2)	139.2 (6)	137.5 (4)
Al(1)-C(1)-C(2)	101.9 (5)	102.4 (4)	Al(2)-C(4)-C(6)	138.0 (6)	137.9 (5)
Al(2)-C(1)-C(3)	99.7 (5)	99.0 (4)	C(5)-C(4)-Al(1)	144.0 (6)	141.6 (6)
C(3)-C(1)-C(2)	56.3 (5)	55.8 (4)	Al(2)-C(13)-C(14)	142 (1)	
Al(1)-C(4)-C(6)	100.6 (5)	100.5 (6)	Al(2)-C(13)-C(15)	140 (1)	
Al(2)-C(4)-C(5)	100.8 (5)	101.2 (5)	C(14)-C(13)-C(15)	61 (1)	
C(6)-C(4)-C(5)	56.7 (5)	54.6 (5)	C(13)-C(14)-C(15)	56 (1)	
C(1)-C(3)-C(2)	62.4 (5)	62.0 (4)	C(13)-C(15)-C(14)	62.5 (9)	
C(1)-C(2)-C(3)	61.3 (5)	62.1 (4)	Al(2)-C(13)-C(X)		118.6 (8)
C(4)-C(6)-C(5)	61.4 (5)	61.9 (6)	Al(2)-C(13)-C(Y)		138.4 (10)
C(4)-C(5)-C(6)	61.9 (5)	63.3 (6)	Al(2)-C(13)-C(Z)		133.7 (7)
Al(1)-C(7)-C(8)	118.6 (6)	118.6 (5)	C(X)-C(13)-C(Y)		64.4 (10)
Al(1)-C(7)-C(9)	117.6 (6)	116.6 (6)	C(X)-C(13)-C(Z)		50.8 (6)
C(9)-C(7)-C(8)	58.4 (6)	57.3 (6)	C(Z)-C(13)-C(Y)		82.7 (10)
C(7)-C(9)-C(8)	61.0 (6)	62.8 (6)	C(13)-C(Z)-C(Y)		47.0 (7)
C(7)-C(8)-C(9)	60.6 (5)	59.9 (6)	C(13)-C(X)-C(Y)		48.5 (8)
Al(1)-C(10)-C(11)	122.6 (7)	123.6 (6)	C(13)-C(X)-C(Z)		55.2 (7)
Al(1)-C(10)-C(12)	127.5 (7)	125.7 (6)	C(13)-C(Y)-C(X)		67.1 (10)
C(11)-C(10)-C(12)	60.5 (6)	59.0 (5)	C(13)-C(Y)-C(Z)		50.2 (8)
C(10)-C(11)-C(12)	59.5 (6)	60.5 (5)	C(13)-C(Z)-C(X)		74.0 (9)
C(10)-C(12)-C(11)	60.0 (6)	60.5 (5)	C(X)-C(Y)-C(Z)		45.1 (7)
Al(2)-C(16)-C(17)	120.5 (6)	121.9 (5)	C(X)-C(Z)-C(Y)		59.4 (10)
Al(2)-C(16)-C(18)	120.2 (5)	119.4 (5)	C(Y)-C(X)-C(Z)		75.5 (12)

Table IV. Comparison of Structural Parameters for the Known Organoaluminum Compounds

compd	Al-C-Al, deg	C_t-Al-C_t, deg	Al-C_b, Å	Al-C_t, Å	Al-Al, Å	C_b-Al-C_b, deg
$[Me_3Al]_2$ [a]	75.7 (1)	123.2 (1)	2.12	1.95 (av)	2.606	104.3 (1)
Me_5Al_2NPh [b]	78.92 (17)	117.20	2.142	1.94	2.723	94.70
$[Me_2AlPh]_2$ [c]	77.4	121.0 (4) 121.5 (4)	2.134 (5)	1.979 (6)	2.683 (3)	101.8 (2)
$[Ph_3Al]_2$ [d]	76.5 (2)	115.4 (2)	2.184 (5)	1.960 (4)	2.702 (2)	103.5 (2)
$[Ph_2Al(C{\equiv}CPh)]_2$ [e]	91.73		1.922 2.184	1.94		
$[Me_2AlH]_2$ [f]	102.6 (16)	118.9 (9)	1.676 (19)	1.949 (3)	2.617 (6)	77.4
$[Me_2AlC{\equiv}CMe]_2$ [g]	92.0 (1.0)	120.8 (1.6)	2.05 (115) 2.15 (3)	1.956 (5)		
$[(c\text{-Pr})_3Al]_2$ 22 °C [g]	78.2 (3)	115.2 (3)	2.087 (av)	1.93 (av)	2.618 (3)	96.7 (3)
−67 °C	77.9 (2)	115.5 (3)	2.074 (av)	1.944 (av)	2.607 (3)	97.1 (2)

[a] Reference 2. [b] Reference 3. [c] Reference 5. [d] Reference 4. [e] Reference 7. [f] Almenningen, A.; Anderson, G. A.; Forgaard, F. R.; Haaland, A. *Acta Chem. Scand.* **1972**, *26*, 2315. [g] Reference 9. [h] Reference 8.

the extreme ranges of 1.44–1.56 Å reported for the shortest distance in *anti,cis,cis*-2,2′-dibromocyclopropyl[19] and the longest distance, the 1,2-C-C bond in 1,1,2,2-tetracyano-cyclopropane.[20] Thus it is quite probable that some unusual interactions are occurring in this system.

The initial postulate concerning the stabilization of the cyclopropyl bridge by use of the p orbitals located on the C_α bridging atom with the nonbonding orbitals of the aluminum

(19) Schrumpf, C.; Susse, P. *Chem. Ber.* **1972**, *105*, 3041.

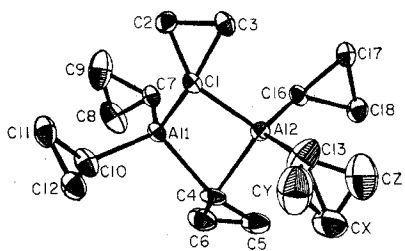(20) Wang, Y.; Stucky, G. D. *Acta Crystallogr., Sect. B* **1973**, *B29*, 1255.

Figure 1. Perspective view of the tricyclopropylaluminum dimer with labeling.

atoms and the subsequent CNDO II calculations which appeared to support this model also predict that the C_α–C_β bond length should increase while the C_β–C_β bond length should decrease with greater double-bond character as indicated in **3**. One

3
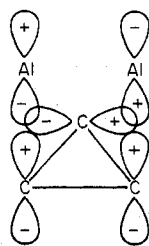
also would predict shortening of the Al–C bridge bond lengths, but, as noted earlier, although the trends in the bond lengths

are in correct direction, the minimal changes observed are not sufficient to be significant.

One might note that similar bond shortening has also been looked for in both cyclopropyl cyanide[21] and cyclopropylacetylene,[22] on the assumption that the C_α–C_x bond should decrease through interaction between the π systems and the p orbitals of the cyclopropyl rings, but was not observed. Thus, one might not expect significant bond shortening in this case either. What does appear to be clear from all of the available data, including the NMR studies cited, the limited CNDO II calculations, and the present structural work, is that the cyclopropyl groups are preferentially located in the bridging positions in the syn configuration and that the Al–C–Al bridge bond appears to be stabilized in some manner by the cyclopropyl ring with the most attractive possibility that of interaction between the p orbitals of the ring carbon and the nonbonding metal orbitals as initially suggested.

Registry No. [Al(c-Pr)$_3$]$_2$, 21892-05-7.

Supplementary Material Available: A listing of observed and calculated structure factor amplitudes (11 pages). Ordering information is given on any current masthead page.

(21) Friend, J. P.; Dailey, B. P. *J. Chem. Phys.* 1958, *29*, 577.
(22) Collins, M. J.; Brutt, C. O.; Boggs, J. E. *J. Chem. Phys.* 1972, *56*, 4262.

Contribution from the Department of Chemistry,
Wayne State University, Detroit, Michigan 48202

Metal–Silicon-Bonded Compounds. 11. Crystal and Molecular Structures of Li$_2$Hg(SiMe$_2$Ph)$_4$ and Li$_2$Hg(SiMe$_3$)$_4$, Novel Chain and Caged Lithium Metallates

WILLIAM H. ILSLEY, MICHAEL J. ALBRIGHT, THOMAS J. ANDERSON, MILTON D. GLICK, and JOHN P. OLIVER*

Li$_2$Hg(SiMe$_2$Ph)$_4$ (I) and Li$_2$Hg(SiMe$_3$)$_4$ (II) crystallize in the space group *C2/c* with four molecules per unit cell. The cell dimensions for I are *a* = 16.269 (5) Å, *b* = 10.298 (3) Å, *c* = 22.390 (6) Å, and β = 110.05 (2)° and for II are *a* = 15.932 (6) Å, *b* = 15.388 (2) Å, *c* = 9.494 (4) Å, and β = 93.53 (3)°. Full-matrix least-squares refinement for I gave final discrepancy factors of R_1 = 0.029 and R_2 = 0.034 for 1677 counter data for which $I > 3\sigma(I)$, while for II, R_1 = 0.026 and R_2 = 0.030 for 1395 counter data for which $I > 2.5\sigma(I)$. The structure of molecule I consists of discrete formula units with the mercury on a twofold axis of symmetry and with the lithium cations enclosed in a cage of silicon and carbon atoms. The mercury–silicon distances are 2.549 (2) and 2.493 (2) Å, the lithium–mercury distance is 2.58 (1) Å, and the lithium–silicon and lithium–carbon distances are in the range from 2.90 (1) to 3.04 (1) and 2.42 (2) to 2.61 (2) Å, respectively. The crystal structure of II consists of zigzag chains of Li$_2$Hg(SiMe$_3$)$_4$ units. The individual Li$_2$Hg(SiMe$_3$)$_4$ units of the chains are held together by the lithium atoms which serve as bridges between the Hg(SiMe$_3$)$_4$ moieties of the chains. Each Hg(SiMe$_3$)$_4$ fragment has a distorted tetrahedral arrangement of silicon atoms about the mercury with mercury–silicon distances of 2.539 (2) to 2.548 (2) Å; the mercury is on a twofold axis of symmetry. The mercury–lithium distance is 2.57 (1) Å, and the lithium–silicon and lithium–carbon distances are 2.69 (1)–2.87 (1) and 2.32 (1)–2.63 (1) Å, respectively. The interactions of the lithium atoms with carbon, silicon, mercury, and hydrogen atoms are considered, and the implications of these interactions with regard to the bonding in these systems are discussed.

Introduction

The unusual properties of the "ate" derivatives such as LiBMe$_4$, LiAlMe$_4$, and Li$_2$BeMe$_4$ have generated interest in their structures and in the bonding interactions present in these complexes. A number of studies have been undertaken in order to gain insight into the nature of the lithium interactions in this class of compounds. These studies have shown that the solid-state structure of LiAlEt$_4$[1] consists of a chain in which

the lithium atoms bridge two AlEt$_4$ units as depicted in I. In LiBMe$_4$ a more complex structure is observed with the lithium occurring in two kinds of positions, one described in terms of a "normal" electron-deficient bond and the second as a linear Li–C–B bond with an extremely short Li–C bond distance.[2,3]

(1) Gerteis, R. L.; Dickerson, R. E.; Brown, T. L. *Inorg. Chem.* 1962, *3*, 872.